Journal of Ceramic Processing Research. Vol. 3, No. 2, pp. 57~61 (2002)

J O U R N A L O F
Ceramic Processing Research

Magnetic properties of $Nd_2Fe_{14}B/\alpha$-Fe nanocomposite alloys

Jung-Ho Park, Dae-Hoon Lee and Taesuk Jang*
Division of Materials and Chemical Eng., Sunmoon University, Asan city, Choongnam 336-708, Korea

The magnetic properties of $Nd_9Fe_{84}B_7$ alloys melt spun and subsequently annealed under various conditions were investigated. It was found that the melt-spun alloys were fully amorphous when they were spun at and above 35 m/s. After annealing for 5~15 minutes at 650~750°C, all alloys melt spun at 40 m/s were transformed to nanocrystalline mixtures of mainly α-Fe and $Nd_2Fe_{14}B$. The evolution of the two phases tended to be more complete at higher temperatures, above 700°C. In particular, the alloys annealed for 10~15 minutes at 700°C, 7~12 minutes at 725°C, or 5~7 minutes at 750°C exhibited smooth demagnetization curves just like those of the quasi-single phase Nd-Fe-B alloys, suggesting the exchange interaction took place effectively in these alloys. M_r/M_s was more than 70% in the alloys annealed above 700°C. The magnetic properties obtained from an alloy annealed for 5 minutes at 750°C were M_r/M_s=72%, ${}_iH_c$=3.4 kOe, B_r=12.7 kG, and $(BH)_{max}$=14.2 MGOe. The estimated grain sizes of $Nd_2Fe_{14}B$ and α-Fe in the alloy were ~55 nm and ~10 nm, respectively.

Key words: Exchange interaction, Nanocomposite alloys, Coercivity, Remanence, Melt spinning.

Introduction

Nd-Fe-B alloys containing less Nd than for the stoichiometric $Nd_2Fe_{14}B$ compound are usually of no practical use because, under an external applied field, the magnetic behavior of coarse grains of the soft magnetic α-Fe existed excessively in these alloys is independent from that of the hard magnetic $Nd_2Fe_{14}B$, resulting in a very poor energy product. However, α-Fe and $Nd_2Fe_{14}B$ in these alloys can be formed on a nanograin scale simultaneously when the alloys were rapidly quenched into a nanocrystalline state [1] or overquenched into an amorphous state and properly annealed subsequently [2]. Then remanences larger than $M_s/2$ with reasonably high coercivities can be obtained even in the isotropic state due to a strong exchange interaction taking place between the fine grains of the two phases. Such an exchange interaction can also occur between $Nd_2Fe_{14}B$ and the other soft magnetic phase Fe_3B [3, 4]. However, the coercivity obtained from the alloys of this system is usually lower than that in the former, although a high remanence is still achieved, due to the lower Nd content (< 5 at%) in the alloys. Because of this low coercivity that causes a large irreversible loss at elevated temperature, these alloys have not been applied for more general permanent magnet use even though they have very good corrosion resistance. Thus, to make the exchange-coupled alloys more practical, it is necessary to improve the coercivity to a reasonable value without much loss of remanence either by a compositional adjustment or by a process control. In this study, the magnetic properties of $Nd_9Fe_{84}B_7$ alloys melt spun and subsequently annealed at various temperatures and times were investigated to figure out the optimum quenching and annealing conditions that ensure solid exchange interaction between α-Fe and $Nd_2Fe_{14}B$.

*Corresponding author:
Tel : +82-41-530-2341
Fax: +82-41-544-1857
E-mail: tsjang@email.sunmoon.ac.kr

Experimental Procedures

The $Nd_9Fe_{84}B_7$ alloys were prepared by arc melting under a high-purity argon atmosphere. The purity of the constituent elements were 99.9% for Fe and Nd, and 99.5% for B. They were crushed into several pieces and remelted by induction melting in a quartz tube with an orifice 0.5 mm in diameter. Then, melt-spun ribbons were obtained by ejecting the molten alloy through the orifice onto a rotating copper wheel under an argon atmosphere. The wheel speed was varied from 30 to 45 m/s to inspect the degree of amorphization in the as-spun state. After inspection of the amorphization, the ribbons melt spun at 40 m/s, which were fully amorphous with thicknesses of 20~25 m and widths of 1.5~2.0 mm, were annealed in evacuated and sealed quartz capsules for 5~15 minutes at 650~750°C; then the capsules were quenched in water.

The composition of the melt-spun ribbons was verified by inductively coupled plasma (ICP) method, and phase identification of both the as-spun and the annealed ribbons was carried out by X-ray diffraction using Cu K_α radiation. The average grain size was estimated by analysing the diffraction peaks using the Scherrer formula. The magnetic properties of the ribbons were measured at room temperature with a vibrating sample magnetometer (VSM) with a maximum applied field of 20 kOe. Several pieces of ribbon were stacked and fixed in parallel for the measurement, then the field was applied parallel to the ribbon surfaces. The demagnetization factor for the measurements was not considered.

Results and Discussion

Figure 1 shows the x-ray diffraction patterns of as-spun ribbons. The ribbons became fully amorphous as the wheel speed increased above 35 m/s. At 30 m/s, however, small amounts of α-Fe and $Nd_2Fe_{14}B$ were still present in a crystalline form. Obtaining a fully amorphous state as a homogeneous precursor is important for crystallographically coherent formation of nanocrystalline hard magnetic phases and soft magnetic phases simultaneously, which insures a strong exchange coupling between the two phases [4]. Such magnetic exchange interaction can also take place in as-spun nanocrystalline ribbons [1]; but it is not easy to adjust the magnetic properties by a thermal treatment because those previously formed fine grains may grow very quickly upon the heat treatment. Therefore, the ribbons spun at 40 m/s, which were fully amorphous in the as-spun state, were used for annealing treatments in this study.

Typical diffraction patterns of the annealed ribbons are shown in Fig. 2. All specimens annealed for 5~15 minutes at 650~750°C were mainly composed of α-Fe and $Nd_2Fe_{14}B$, regardless of the annealing temperature and time, although the crystallization and distribution of the phases were somewhat different from each other. At relatively low temperatures, 650~675°C, the formation of α-Fe and $Nd_2Fe_{14}B$ was insufficient even after 15 minutes, providing some broad and unresolved diffraction peaks of α-Fe and $Nd_2Fe_{14}B$. It is highly likely that other soft magnetic phases such as the $TbCu_7$ type phases, $Nd_2Fe_{23}B_3$, and Fe_3B [2, 5, 6] were also formed in this temperature range although they were not completely identified in the diffraction patterns. Except for Fe_3B that can be also magnetically coupled with

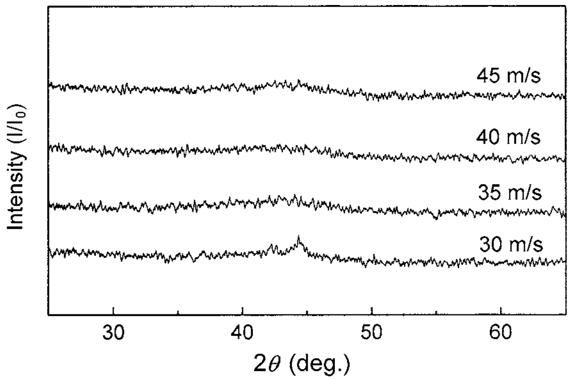

Fig. 1. X-ray (Cu *K*) diffraction patterns of the as-spun $Nd_9Fe_{84}B_7$ alloys.

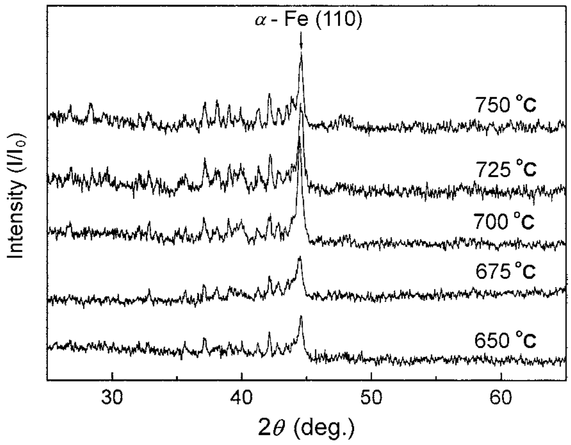

Fig. 2. X-ray (Cu *K*) diffraction patterns of $Nd_9Fe_{84}B_7$ alloys melt spun at 40 m/s and subsequently annealed for 5 minutes at 650~750°C.

$Nd_2Fe_{14}B$, these soft magnetic phases will behave as non-interacting particles which deteriorate the magnetic properties [2, 6] (See Fig. 3a). Above 700°C, on the other hand, the formation of α-Fe and $Nd_2Fe_{14}B$ was more complete. The average grain size of $Nd_2Fe_{14}B$ and α-Fe in the ribbons annealed for 10~15 minutes at 700°C, 7~12 minutes at 725°C, or 5~7 minutes at 750 °C was 40~60 nm and ~10 nm, respectively. However, the grain size of $Nd_2Fe_{14}B$ and α-Fe in the ribbons annealed for 15 minutes at 725°C or for more than 10 minutes at 750°C was larger than the former, indicating the grain growth of both $Nd_2Fe_{14}B$ and α-Fe. The diffraction patterns of the ribbons annealed for 5~7 minutes at 700°C and 5 minutes at 725°C were similar to those annealed below 700°C. As a whole, the annealing temperature should be above 700°C as was claimed in Ref. [2], but the proper range of annealing time tended to be reduced as the annealing temperature increased, *i.e.*, 10~15 minutes at 700°C, 7~12 minutes at 725°C, and 5~7 minutes at 750°C. Fe_3B that was claimed to exist in the ribbons annealed above 700°C [2] but was not confirmed in the ribbons treated by a rapid thermal annealing (RTA) [5] was not detected in our specimens also.

Because the magnetic exchange coupling between a soft magnetic (α-Fe) phase and a hard magnetic ($Nd_2Fe_{14}B$) phase depends on the grain size and distribution of the phases, the shape of hysteresis loops of nanocrystalline alloys is sensitively influenced by the formation of the phases from the homogeneous precursor, *i.e.*, by annealing. Figure 3 shows typical hysteresis loops obtained from the annealed ribbons. When the ribbons were annealed below 700°C or for 5 minutes at 700~725°C, their M(H) curves always exhibited a small kink at low fields as illustrated in Fig. 3a. That is, the magnetic transition at a low field was abrupt, mainly due to the unfavorable soft magnetic phases which did not interact properly with the hard magnetic $Nd_2Fe_{14}B$ grains. As mentioned earlier, α-Fe

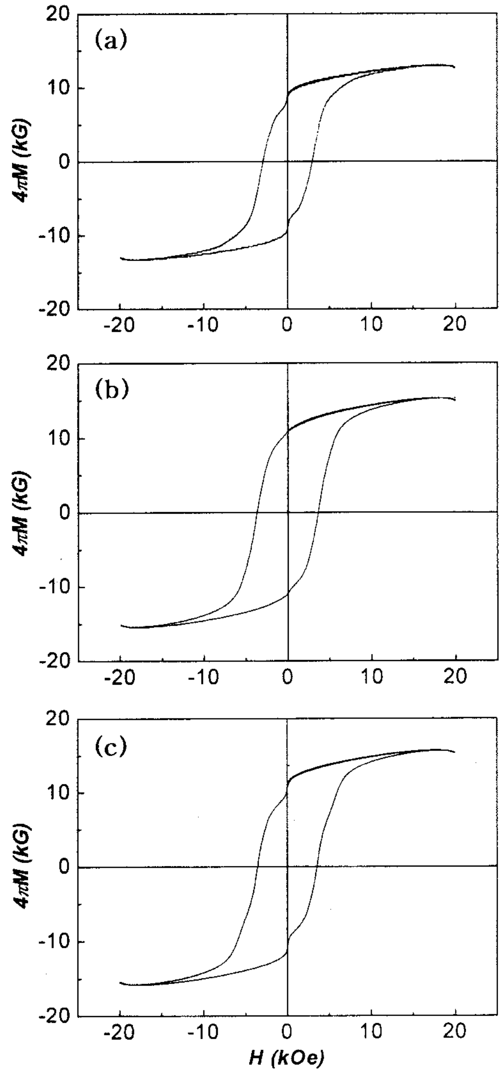

Fig. 3. Hysteresis loops of the annealed $Nd_9Fe_{84}B_7$ alloys; (a) Under annealed (650°C/7 minutes), (b) optimally annealed (750 °C/7 minutes), and (c) over annealed (750°C/15 minutes). All melt spun at 40 m/s.

and $Nd_2Fe_{14}B$ did not develope well at 650~675°C, and it is believed that other soft magnetic $TbCu_7$-type phases and $Nd_2Fe_{23}B_3$ known to crystallize simultaneously in this temperature range [2, 6] and to behave as noninteracting particles were responsible for the kink in the loop. As typically shown in Fig. 3b, on the other hand, the ribbons annealed for 10~15 minutes at 700 °C, 7~12 minutes at 725°C, or 5~7 minutes at 750°C exhibited smooth transitions in their demagnetization curves, just like those of the quasi-single phase Nd-Fe-B alloys, implying the exchange interaction took place effectively. However, when the ribbons were annealed for 15 minutes at 725°C or 10~15 minutes at 750°C, the kink appeared again on the loops as shown in Fig. 3c. This is probably due to the grain growth of α-Fe because the above mentioned soft magnetic phases should decompose completely at these temperatures [2]. In fact, the grain size of α-Fe, and also of $Nd_2Fe_{14}B$, measured from these ribbons was somewhat larger than that of the properly annealed ones. Not only an overgrowth of the soft magnetic phase but also more generally a non-uniform distribution of the phases would cause a kink on the demagnetization curve [5]. Magnetic field annealing and a subsequent stress relief treatment would help to remove the kink and thereby enhance the magnetic properties [7].

Magnetic properties measured from the annealed ribbons are summarized in Table 1. The alloys annealed at and above 700°C generally yielded higher magnetic values than those annealed below 700°C due to, as mentioned earlier, more complete formation of nano-crystalline α-Fe and $Nd_2Fe_{14}B$. However, the alloys that showed a kink on the demagnetization curves, *i.e.*, the alloys annealed for 5 minutes at 700°C and at 725 °C, or the alloys annealed for 10~15 minutes at 750°C exhibited lower energy products than those annealed at the corresponding temperatures. It is believed that insufficient development of the two phases is responsible primarily for the former while overgrowth of the soft phase is responsible for the latter. It is interesting to note that the ribbon alloy annealed for 15 minutes at 725°C exhibited higher remanence and energy product values even though it showed a kink on the demagnetization curve. This implies that an even distribution of α-Fe and $Nd_2Fe_{14}B$ grains unless they are of nano scale would be more important than the size of the soft magnetic phase itself to determine the overall exchange coupling effect. Unfortunately, the coercivity values of the annealed ribbons were all lower than those of the optimally quenched ribbons [1]. This is thought to be due to larger grains of α-Fe and $Nd_2Fe_{14}B$ inevitably accompanied by the annealing of overquenched ribbons at the relatively high temperatures, above 700°C, to decompose the metastable non-interacting soft magnetic $TbCu_7$-type phases and $Nd_2Fe_{23}B_3$ completely [2]. An investigation using a transmission electron microscope is necessary for more detailed analysis. The highest energy product obtained in this study was 14.2 MGOe with ${}_iH_c$=3.4 kOe and B_r=12.7 kG, measured from the ribbons annealed for 5 minutes at 750°C. The average grain size of α-Fe and $Nd_2Fe_{14}B$ in this alloy was estimated to be ~10 nm and ~60 nm, respectively, and the volume fraction of $Nd_2Fe_{14}B$ was 68% estimated by a simple approximation of the saturation magnetization [4].

The remanence ratios (m_r) of the annealed ribbons, as shown in Table 1, were all greater than 0.5 which is expected from an isotropic body of non-interacting single domain particles with uniaxial anisotropy; suggesting that the exchange coupling between soft magnetic and hard magnetic phases was acting effectively although the formation and distribution of the phases did not seem to be ideal. In particular, the m_r values of the alloys annealed at and above 700°C were mostly above 0.7. Enhancement of the remanence arises from exchange

Table 1. Magnetic properties of α-Fe/$Nd_2Fe_{14}B$ nanocomposite $Nd_9Fe_{84}B_7$ alloys

Annealing Temp. (°C)	Annealing Time (min.)	$_iH_c$ (kOe)	B_r (kG)	$(BH)_{max}$ (MGOe)	m_r
650	5	2.5	10.5	9.3	0.67
	7	2.9	9.0	7.3	0.69
	10	2.6	9.1	7.8	0.67
	12	2.6	8.6	8.3	0.69
	15	2.7	10.8	9.8	0.68
675	5	2.6	9.2	8.5	0.68
	7	2.7	10.2	9.5	0.68
	10	2.6	8.9	8.3	0.69
	12	2.6	8.2	8.0	0.68
	15	2.7	10.6	9.8	0.69
700	5	3.2	10.8	8.2	0.70
	7	2.8	10.7	10.8	0.70
	10	3.0	11.5	10.7	0.70
	12	3.1	11.3	11.8	0.71
	15	3.5	12.8	13.8	0.72
725	5	2.9	10.3	9.5	0.69
	7	3.1	10.8	10.8	0.72
	10	3.2	10.9	12.0	0.72
	12	3.5	11.1	12.5	0.71
	15	3.4	11.5	12.8	0.72
750	5	3.4	12.7	14.2	0.72
	7	3.7	10.9	13.0	0.71
	10	3.4	11.2	12.5	0.72
	12	3.4	9.8	10.5	0.71
	15	3.6	11.0	11.5	0.70

coupling of magnetic moments across the interface between hard magnetic and soft magnetic grains, leading to the magnetic moment of the soft magnetic phase being aligned with that of the hard magnetic one. As a consequence, there is a large degree of reversibility in the demagnetization process [4].

Figure 4 shows a recoil curve of the ribbons whose m_r is 0.72. The recoil behavior to zero magnetization was similar to that with the optimum microstructure, $b_m = b_{cm}$ [4], although the average grain size of the $Nd_2Fe_{14}B$ was quite large, ~60 nm. This is thought to originate from the small grain size of α-Fe that was still estimated to be the ideal value of about 10 nm. Therefore, the nucleation field (H_{no}) of this alloy is expected to be close to the value of the coercivity.

Conclusions

Melt-spun $Nd_9Fe_{84}B_7$ alloys were fully amorphous when they were spun at and above 35 m/s. After annealing for 5~15 minutes at 650~750°C, all alloys melt spun at 40 m/s were mainly composed of nano-crystalline α-Fe and $Nd_2Fe_{14}B$. However, evolution of the two phases tended to be complete at higher temperatures, above 700°C. In particular, the alloys annealed for 10~15 minutes at 700, 7~12 minutes at 725°C, or 5~7 minutes at 750°C exhibited a smooth transition in their demagnetization curves just like those of the quasi-single phase Nd-Fe-B alloys, suggesting the exchange interaction took place effectively. M_r/M_s (=m_r) was more than 0.7 in the alloys annealed above 700 °C. The magnetic properties obtained from an alloy annealed for 5 minutes at 750°C were m_r=0.72, $_iH_c$= 3.4 kOe, B_r=12.7 kG, and $(BH)_{max}$=14.2 MGOe. The estimated grain size of $Nd_2Fe_{14}B$ and α-Fe in the alloy was ~55 nm and ~10 nm, respectively. Lower coercivities seemed to be attributed to an uneven distribution of somewhat larger grains of the two phases.

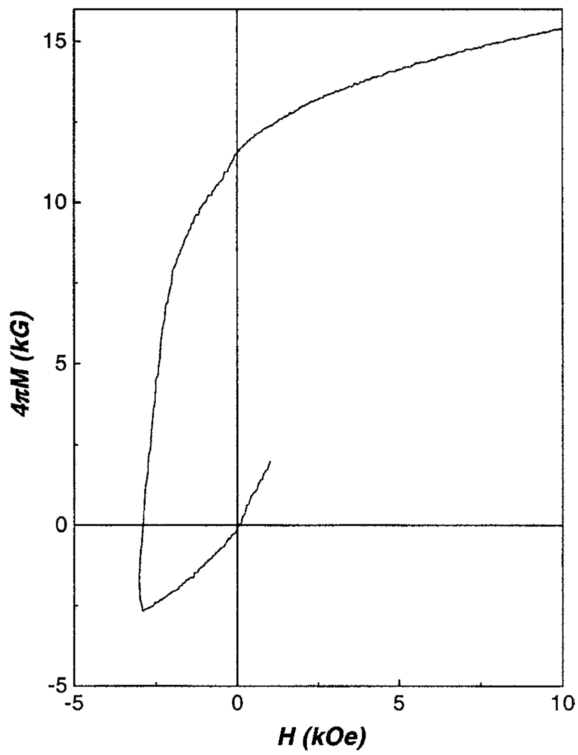

Fig. 4. Recoil curve of $Nd_9Fe_{84}B_7$ alloy melt spun at 40 m/s and subsequently annealed for 10 minutes at 725°C.

Acknowledgements

This work was supported by grant No. 2000-1-30100-015-3 from the Basic Research Program of the Kores Science and Engineering Foundation.

References

1. A. Manaf, R.A. Buckley, and H.A. Davies, J. Magn. Magn. Mater. 128 (1993) 302-306.
2. A.M. Gabay, A.G. Popov, V.S. Gaviko, Ye.V. Belozerov, and A.S. Yermolenko, J. Alloys Compd. 245 (1996) 119-124.
3. R. Coehoorn, D.B. DeMooij, and C. de Waard, J. Magn. Mgn. Mater. 80 (1989) 101-104.
4. E.F. Kneller and R. Hawig, IEEE Trans. Magn. 27 (1991)

3588-3600.
5. J.S. Fang, M.F. Hsieh, S.K. Chen, and T.S. Chin, Jpn. J. Appl. Phys. 36 (1997) 6316-6324.
6. A.M. Gabay, A.G. Popov, V.S. Gaviko, Ye.V. Belozerov, A.S. Yermolenko, N.N. Shchegoleva, J. Alloys Compd. 237 (1996) 101-107.
7. H. Chiriac, M. Marinescu, K.H.J. Buschow, F.R. de Boer, E. Bruck, J. Magn. Magn. Mater. 202 (1999) 22-26.